International Journal of Research
Available at https://edupediapublications.org/journals
e-ISSN: 2348-6848
p-ISSN: 2348-795X
Volume 05 Issue 12
April 2018

Hormonics Compensation in an Islanded Ac Microgrid by an Enhanced Power Sharing Scheme

M.Sreedhar & Rajesh Thota
[1]m.Tech, Vaagdevi College Of Engineering, Bollikunta, Warangal.
[2]associate Professor, Vaagdevi College Of Engineering, Bollikunta, Warangal.

,

Abstract—*In this paper, proposes Power sharing problems are associated with DG reactive power, imbalance power and harmonic power. To address unequal power sharing problems an enhanced hierarchical control structure with multiple current loop damping schemes for voltage unbalance and harmonics compensation (UHC) in ac islanded microgrid is proposed. An enhanced droop control method through online virtual impedance adjustment is used to solve power sharing problems. With the regulation of DG virtual impedance at fundamental positive sequence, fundamental negative sequence, and harmonic frequencies, an accurate power sharing can be realized at the steady state.. By using the proposed unbalance and harmonics compensation, the auxiliary control, and the virtual positive/negative-sequence impedance loops at fundamental frequency, and the virtual variable harmonic impedance loop at harmonic frequencies, an accurate power sharing is achieved. Moreover, the low bandwidth communication (LBC) technique is adopted to send the compensation command of the secondary control and auxiliary control from the microgrid control center to the local controllers of DG unit. By using the simulation results we can analyze the proposed method.*

Index Terms—Auxiliary control, distributed generation, droop control, microgrid, power sharing, secondary control, voltage unbalance and harmonics compensation, virtual impedance.

INTRODUCTION

In this control category, real power and reactive power in the power control loop are calculated using low pass filters (LPF). The reactive power sharing performance is dependent on the impedance of DG feeders. In a DG unit is equipped with dominate inductive virtual impedance the reactive power sharing errors can be reduced. The proposed control system of the microgrid mainly consists of the positive sequence real and reactive power droop controllers, voltage and current controllers, the selective virtual impedance loop, the unbalance and harmonics compensators, the secondary control for voltage amplitude and frequency restoration, and the auxiliary control to achieve a high-voltage quality at the point of common coupling.

Compared to the conventional distribution system, the microgrid can operate in both grid-connected and autonomous islanding modes, offering more reliable power to the critical loads. In the islanded mode, each DG unit should be able to supply certain amount of the total load proportional to its power rating. To achieve the power sharing requirement with only local measurement and eliminating an external high bandwidth communication links among the DG units, the frequency and voltage droop control methods are analyzed.

To enhance the performance of the microgrid the virtual impedance aided DG operation is considered. It is well known that the primary control, which contains droop control, voltage and current controllers and virtual impedance loop, does not require high bandwidth communication, and the secondary control is often adopted in order to achieve global controllability of the microgrid [16]. Therefore, a microgrid should be able to operate under unbalanced and nonlinear load conditions without performance degradations.

In order to overcome the power quality problems, the series active power filters (APFs) can be utilized to compensate the voltage unbalance and harmonics by injecting negative sequence and harmonic voltage to the distribution line through coupling transformers

In this paper, an enhanced hierarchical control methodology is applied to DG units in an islanded microgrid. The selective virtual impedance at the fundamental positive sequence, fundamental negative sequence, and harmonic frequencies are adopted to achieve better power sharing of reactive, unbalance and harmonic powers.

The main aim of this paper are 1) Development of an enhanced hierarchical power sharing method for an islanding microgrid under nonlinear and/or unbalanced load conditions. 2) Implementation of the VPI and VNI loops at fundamental frequency, and the VVHI loop at harmonic frequencies to compensate the reactive, unbalance and harmonic power sharing errors. 3)

II. DECENTRALIZED MICROGRID SYSTEM CONFIGURATION

A typical system configuration of a low-voltage microgrid with n DG units and complex load conditions is given in Fig. 1. The LBC is applied for sending the data information of the secondary controllers and the PCC voltage harmonics from the microgrid control center (MGCC) to the local controller to realize the proposed compensation scheme in DG units in a practical and synchronized manner. Furthermore, a static switch is used to dynamically disconnect the microgrid from the upstream distribution system in case of grid faults.

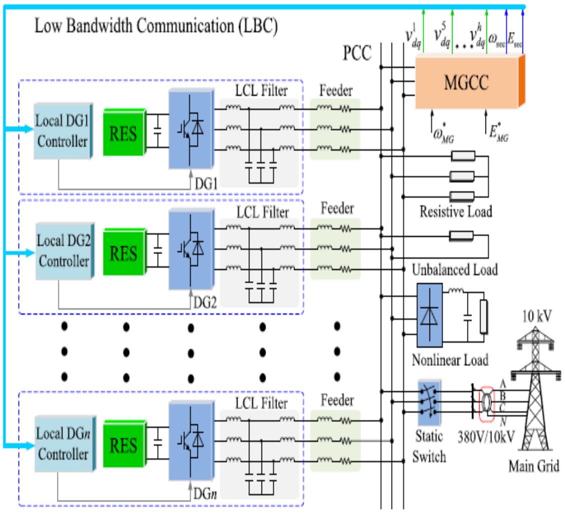

Fig. 1. Typical structure of MG with multiple parallel-connected DG units.

Although the proposed control strategies can operate in either the grid-connected mode or islanded mode, only the islanded operation mode will be considered in this paper.

III. DYNAMIC MODEL OF A DG UNIT

The power stage of a DG unit and the proposed hierarchical control strategy for the interface inverter connected in an islanded mode is shown in Fig. 2.

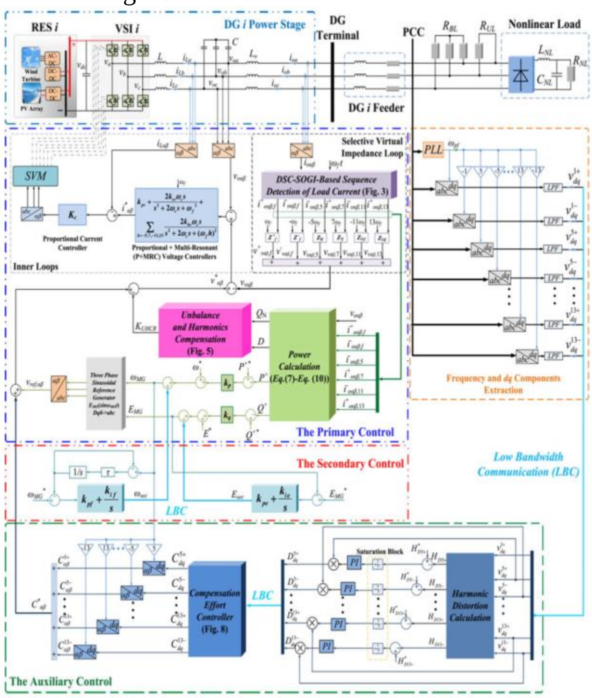

Fig. 2. Block diagram of the proposed hierarchical control strategy for the islanded microgrid.

The DG unit with its LCL filter can be considered as a subsystem of the microgrid. In this section, the dynamic model of a DG unit, as a subsystem of the overall microgrid, is presented. By using Kirchhoff 's Voltage Law and Kirchhoff 's Current Law [35], LC output filter shown in Fig. 2 yields the following differential equations

$$\begin{cases} T_T \dfrac{dI_L}{dt} = \dfrac{1}{L} V - \dfrac{1}{L} T_T V_0 \\ C \dfrac{dV_o}{dt} = I_C = I_L - I_0 \end{cases}$$

$$T_T = \begin{bmatrix} 1 & -1 & 0 \\ 0 & 1 & -1 \\ -1 & 0 & 1 \end{bmatrix} \qquad (1)$$

where V = [vab, vbc, vca]T is the inverter output line to line voltage vector, IL = [iLa, iLb, iLc]T is the inverter phase current vector, Io = [ioa, iob, ioc]T is the load phase current vector, IC = [iCa, iCb, iCc]T is the capacitor current vector, V o = [voa, vob, voc]T is the line to neutral voltage vector at the load side. The Clarke transformation is adopted to transform the variables between abc and αβ frames. The state-space equation of the system in the αβ frame is obtained as follows

$$\dot{x_s} = A_s x_s + B_s u_s + D_s w_s y_s = F x_s \qquad (2)$$

IV. PROPOSED HIERARCHICAL CONTROL STRATEGY

As shown in Fig. 2, the error signals obtained by comparing the measured output voltage, the voltage drop generated by the selective virtual impedance loop, the power controllers, the selective harmonics compensation of PCC, the UHC block, and the reference value which are regulated by the proportional plus multi-resonant controllers (P+MRC) to generate references for the current loop. The proposed hierarchical control strategies are presented as follows.

A. The Primary Control

1) Power Droop Control Loop: The three-phase instantaneous real power (p) and reactive power (q) are calculated from αβ-axis output voltage (vCαβ) and output current (ioαβ) as

$$p = v_{0\alpha} i_{0\alpha} + v_{0\beta} i_{0\beta}$$

$$q = v_{0\beta} i_{0\alpha} - v_{0\alpha} i_{0\beta} \qquad (3)$$

Each of the instantaneous powers calculated using (5) and (6) consists of dc and ac components. The ac parts are fundamental positive-sequence active and reactive powers that can be extracted using low pass filters (LPFs). The ac parts are generated by the unbalance and harmonic components of the output voltages and currents.

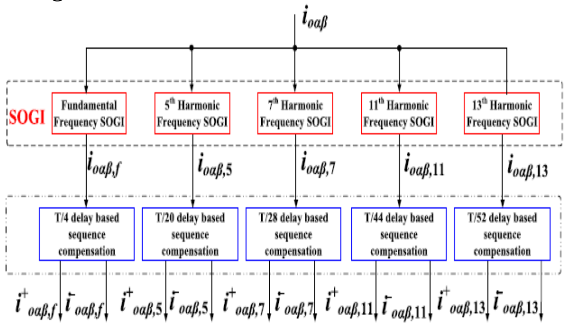

Fig. 3. DSC-SOGI based sequence decomposition of fundamental positive sequence, fundamental negative sequence, and harmonic components.

A simplified detection diagram of the DSC-SOGI based sequence decomposition is depicted in Fig. 3. At a local DG unit controller, the droop control is utilized to avoid communication wires while obtaining good power sharing, which is responsible for adjusting the frequency and amplitude of the voltage reference according to the positive sequence real and reactive powers (P+ and Q+), ensuring P+ and Q+ flow control [16], [18]. The positive sequence real power-frequency (P+ − ω) and reactive power-voltage magnitude (Q+ − E) droop controllers are defined as

$$\omega = \omega^* - k_p(P^+ - P^{+*})$$

$$E = E^* - k_q(Q^+ - Q^{+*}) \qquad (4)$$

where ω and E represent the frequency and amplitude of the output voltage reference, ω∗ and E∗ are the nominal frequency and amplitude, P+∗ and Q+∗ are the fundamental positivesequence real and reactive power references normally set to zero in islanded microgrid, and kp and kq are droop coefficients.

2) DSC-SOGI Based Selective Virtual Impedance Loop:

Virtual resistance enhances system damping without adding additional power loss, since it is realized by a control loop and it is possible to implement without decreasing system efficiency. Moreover, the virtual inductance is utilized to make the DG output impedance more inductive to improve decoupling of P and Q, thus enhances the system stability, and reduces power oscillations and circulating currents. As shown in Fig. 4, the voltage drop across the VPI, VNI and VVHI loops in αβ reference frame are

$$VP_{loop}: \begin{bmatrix} v^+_{va,f} \\ v^+_{v\beta,f} \end{bmatrix} = \begin{bmatrix} R^+_{v,f} & -\omega_f L^+_{v,f} \\ \omega_f L^+_{v,f} & R^+_{v,f} \end{bmatrix} \begin{bmatrix} i^+_{o\alpha,f} \\ i^+_{o\beta,f} \end{bmatrix} \qquad (5)$$

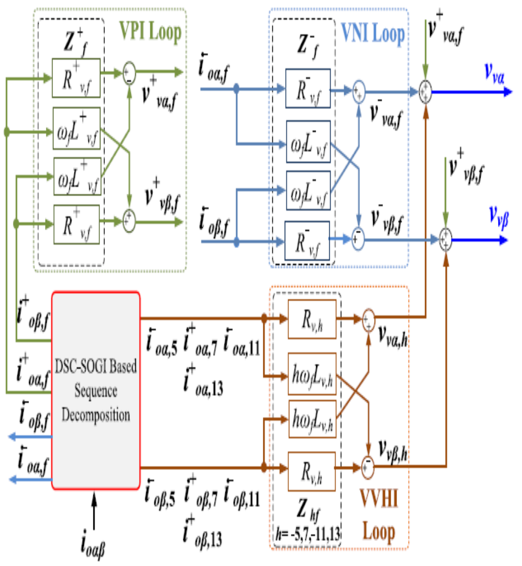

Fig. 4. Block diagram of DSC-SOGI-based selective virtual impedance loop.

3) Local Unbalance and Harmonics Compensation Scheme:

It is well known that voltage unbalance and harmonics leads to the appearance of the negative sequence and harmonic components. Thus, the compensation of the voltage unbalance and harmonics can be achieved by reducing the negative sequence and harmonics voltages. As shown in Fig. 2, the output of the unbalance and harmonics compensation block [unbalance and harmonics compensation reference (KUHCR)] is injected as a reference for the voltage controller. As shown in Fig. 5, the fundamental negative sequence reactive power (QN) and the fundamental harmonic components

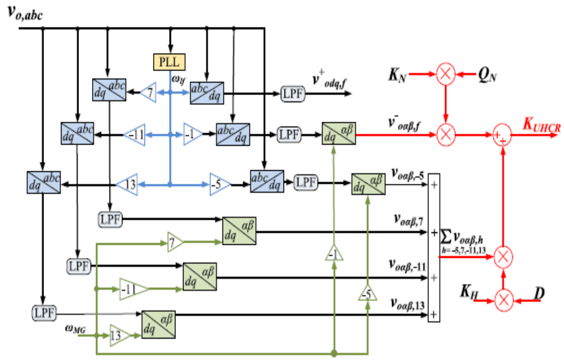

Fig. 5. Block diagram of the local unbalance and harmonics compensation

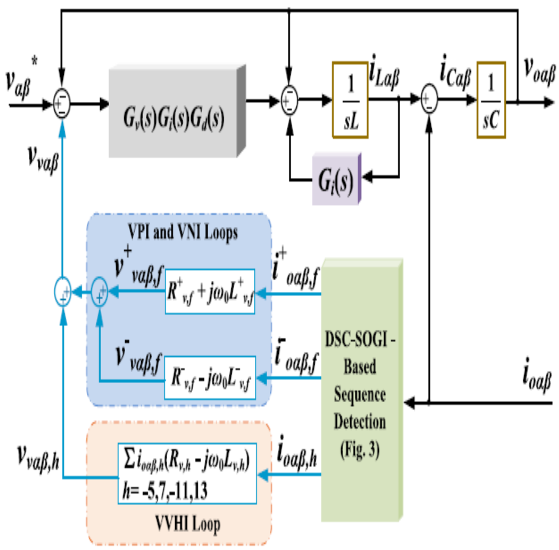

Fig. 6. Simplified diagram of the voltage and current loops integrated with virtual impedance loop.

reactive power (D) are multiplied by two constant values (KN and KH), and also by the instantaneous fundamental negative sequence voltage (v − oαβ,f) and the total harmonics voltage (voαβ,h) to generate this compensation reference, then the KUHCR can be described as

$$K_{UHCR} = K_N.Q_N v_{o\alpha\beta,f} + K_H.D.\sum_{h=5,7,11,13} v^{\pm}_{0\alpha\beta,h} \quad (6)$$

where the coefficients KN and KH are designed to ensure that the voltage unbalance and harmonics are compensated to an acceptable level without violating the system stability. With the UHC method, the harmonic and unbalance power sharing errors can be effectively compensated. Notably, the values of the KN and KH should also ensure the stability of the islanded microgrid system.

4) Inner Voltage and Current Control Loops:

The voltage loop reference signals are modified by the virtual impedance loop, which contains the VPI, VNI, and VVHI loops, as shown in Fig. 6. The output voltage of a DG unit can be derived as

$$v_{0\alpha\beta}(S) = G(s)v^*_{\alpha,\beta} - \left(G(s)Z_{v\alpha\beta}(s)\right) + Z_{o\alpha\beta}(s)i_{0\alpha\beta} \quad (7)$$

where G(s), Zvαβ , and Zoαβ are the closed-loop voltage transfer function, resistive-inductive virtual impedance, and the output impedance without virtual impedance loops, respectively.

The total output impedance with the virtual impedance loop can be derived as

$$Z_{C\alpha\beta}(s) = G(s)(Z^+_{v\alpha\beta,f}) + Z_{v\alpha\beta,h}(s) + Z_{0\alpha\beta}(s) \quad (8)$$

B. The Secondary Control

In order to mitigate the problem of the inherent trade-off between power sharing and voltage and frequency regulation of the droop method, a restoration control is added to remove any steady-state error introduced by the droop controller and achieve global controllability of the microgrid that ensures nominal values of voltage amplitude and frequency under load disturbances and harmonics. The secondary control is realized by LBC link among the DG units. By using this approach, the frequency and voltage amplitude restoration compensators can be represented as

$$\omega_{ssc} = k_{pf}(\omega^*_{MG} - \omega_{MG}) + k_{if}\int(\omega^*_{MG} - \omega_{MG})dt$$

$$E_{ssc} = k_{pe}(E^*_{MG} - E_{MG}) + k_{ie}\int(E^*_{MG} - E_{MG})dt \quad (9)$$

where kpf , kif , kpe , and kie are the control parameters of the proportional integral (PI) compensator of the frequency and voltage restoration control, respectively.

The control signal (Esce) is sent to the primary control level of each DG in order to remove the steady-state errors of the droop controller. Fig. 7 shows the operation principle of the secondary control, which removes frequency and voltage amplitude deviation caused by primary controller. The characteristic of secondary control for frequency restoration is shown in Fig. 7(a).

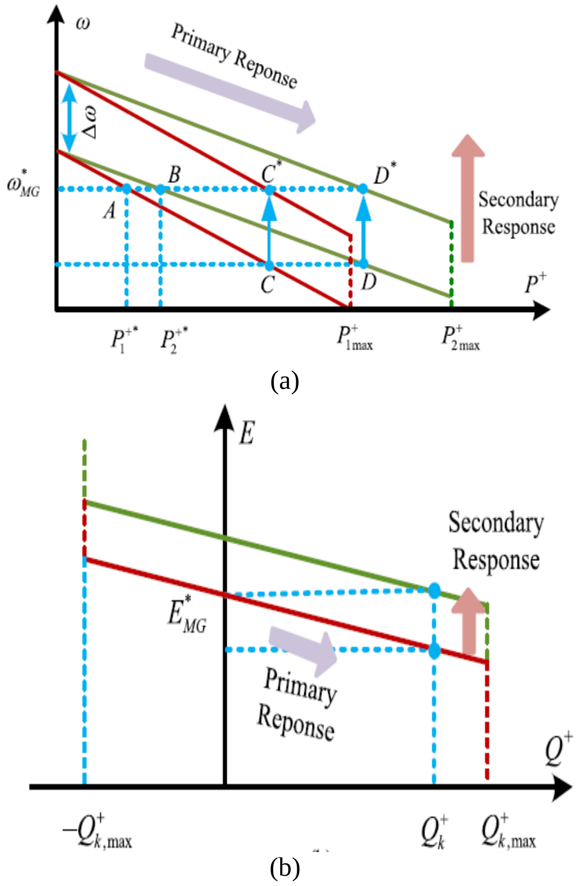

Fig. 7. Secondary control versus primary control response. (a) Frequency restoration. (b) Voltage amplitude restoration.

It can be seen that secondary control shifts up the primary response so that frequency reaches to the nominal value. As shown in Fig. 7(a), the points of A and B are the nominal frequencies of the DG1 and DG2, respectively. The operation points of DG1 and DG2 deviate from the nominal frequencies and operate at the points of C and D when a transient increase of load is applied in the system. The idling frequency changes and the operation points of DG1 and DG2 shift to new operating points of C∗ and D∗ after the secondary controller is applied in the control

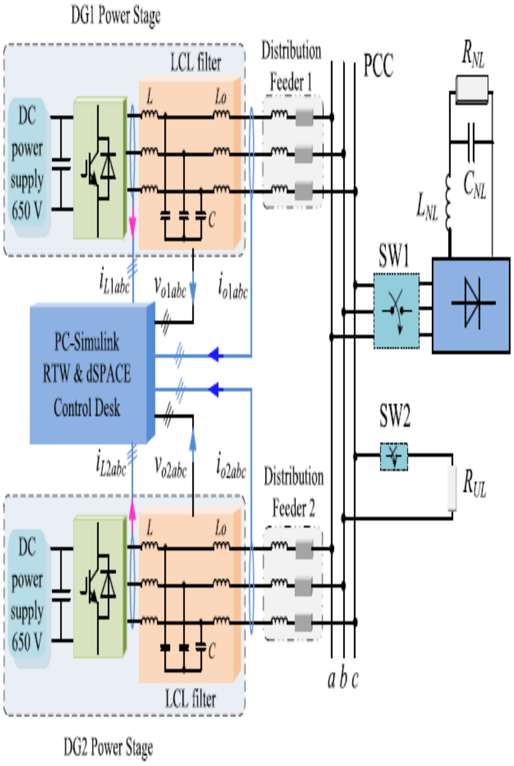

Fig. 9. Schematic of the test microgrid with two parallel-connected DG units.

TABLE I POWER STAGE AND CONTROL PARAMETERS

System Parameter	Value
LCL filter	$L = L_o = 1.8\text{mH}$ and $C = 25\mu F$
DC link voltage	650 V
Main grid	380 V (line to line *RMS*)/50 Hz
Switching frequency	10 kHz
DG feeder	DG1 feeder inductance and resistance $L_{DG1} = 3\text{mH}$ $R_{DG1} = 0.2W$ DG2 feeder inductance and resistance $L_{DG2} = 1\text{mH}$ $R_{DG2} = 0.2W$
Multi-loop Voltage Control Parameter	**Value**
k_{pv}, k_{rv}	0.175, 200
k_{hv}	$50(h = -5), 40(h = 7), 20(h = -11, 13)$
ω_c	1
k_c	5
Power Control Parameter	**Value**
k_p, k_q	0.0001 rad/s/W, 0.0001 V/Var
$k_{pf}, k_{if}, k_{pe}, k_{ie}$	0.8, 10 s^{-1}, 0.8, 10 s^{-1}
τ	50 ms
K_N and K_H	0.9, 0.4
$R - v, f, R_{v,5}, R_{v,7}$, $R_{v,11}$, and $R_{v,13}$	6, 1, 1, 4 and 4 Ω
$L + v, f, L_{v,5}, L_{v,7}$, $L_{v,11}$, and $L_{v,13}$	6, 2, 1.5, 1.5 and 1.5 mH
Load Parameter	**Value**
R_{UL}	230 Ω
L_{NL}, R_{NL}, C_{NL}	84 μH, 460 Ω, 235 μF

system. Without this action, the frequency of the MG is load dependent. As shown in Fig. 7(b), the secondary control is able to remove voltage deviations caused by primary control in DG unit and the voltage amplitude restoration can be achieved.

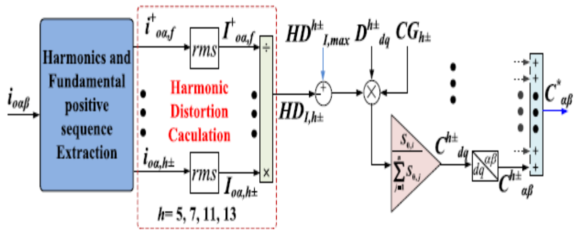

Fig. 8. Block diagram of the compensation effort controller.

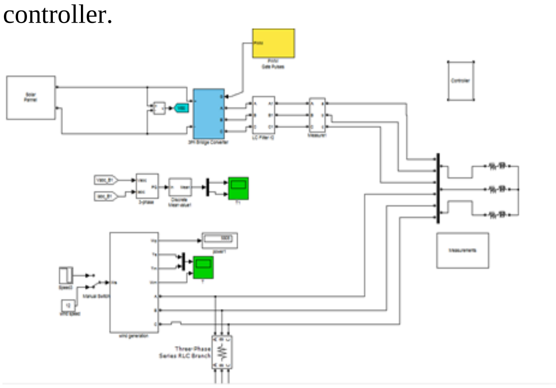

International Journal of Research
Available at https://edupediapublications.org/journals
e-ISSN: 2348-6848
p-ISSN: 2348-795X
Volume 05 Issue 12
April 2018

Fig.9.Block diagram of simulation

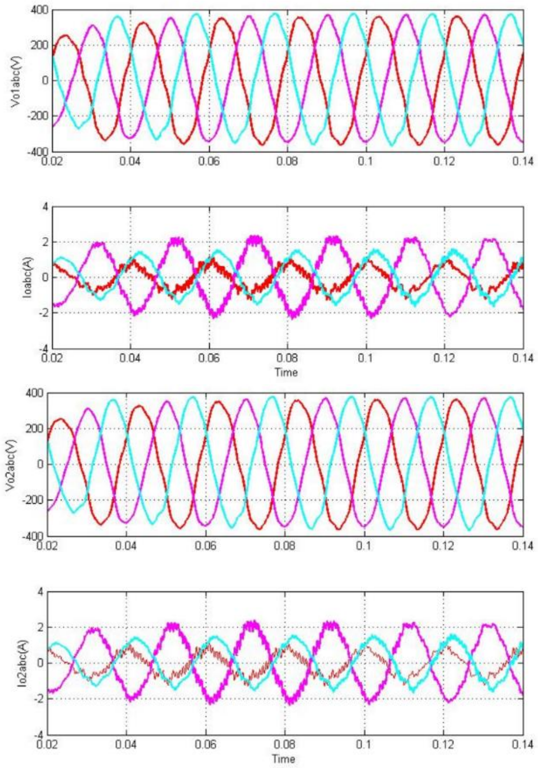

Fig. 10. Performance of the conventional droop control in a microgrid with unbalanced nonlinear load. (a) Output voltages and currents of DG1. (b) Output voltages and currents of DG2.C. The Auxiliary Control

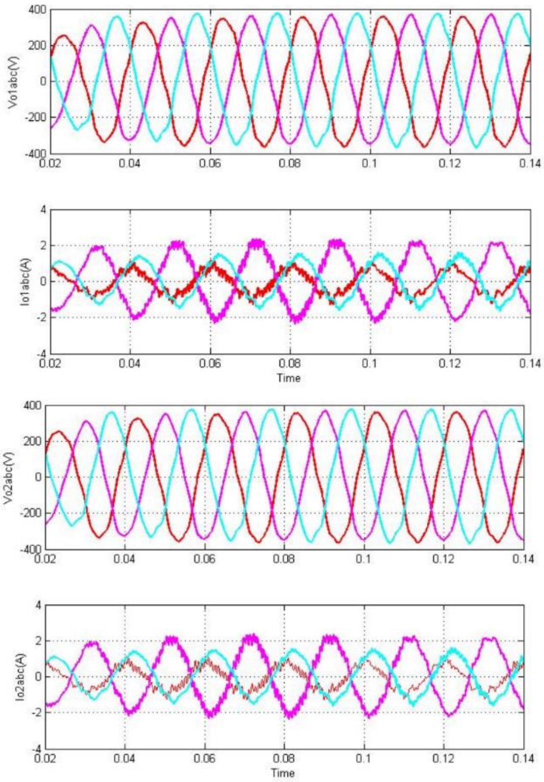

Fig. 11. Performance of the proposed compensation method in a microgrid with unbalanced nonlinear load. (a) Output voltages and currents of DG1. (b) Output voltages and currents of DG2.C. The Auxiliary Control

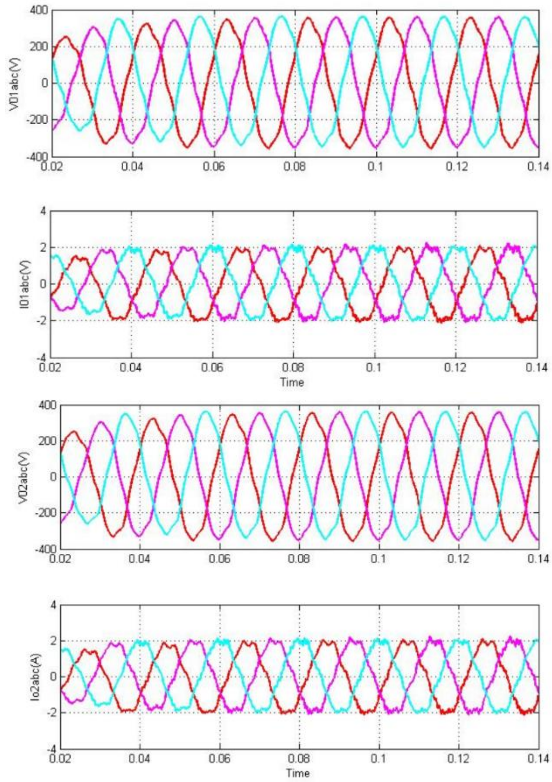

Fig. 12. Performance of the conventional droop control in a microgrid with nonlinear load. (a) Output voltages and currents of DG1. (b) Output voltages and currents of DG2.

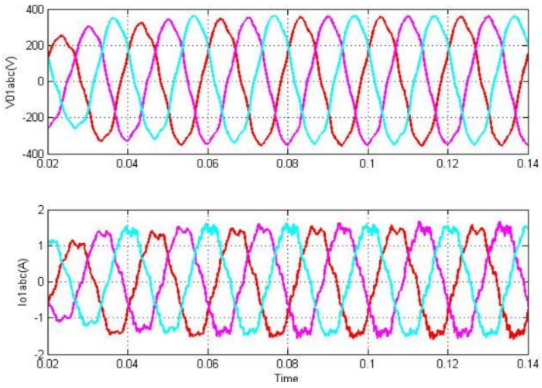

e-ISSN: 2348-6848
p-ISSN: 2348-795X
Volume 05 Issue 12
April 2018

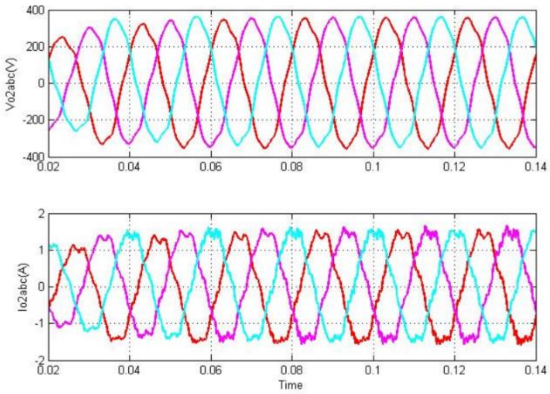

Fig. 13. Performance of the proposed compensation method in a microgrid with nonlinear load. (a) Output voltages and currents of DG1. (b) Output voltages and currents of DG2.

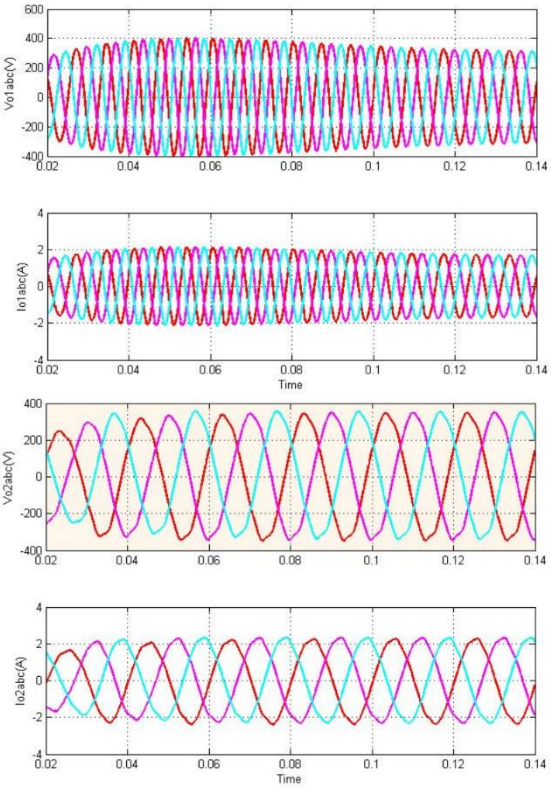

Fig. 14. Performance of the conventional droop control method in a microgrid with unbalanced resistive load plus nonlinear load. (a) Output voltages and currents of DG1. (b) Output voltages and currents of DG2.

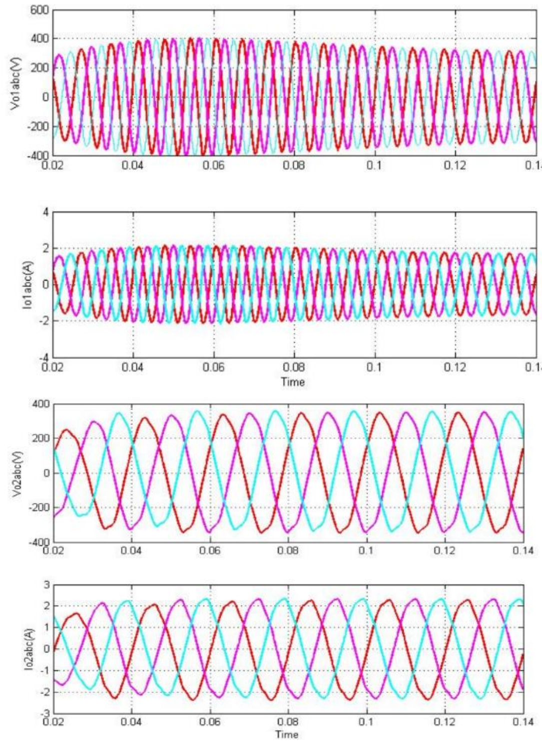

Fig. 15. Performance of the proposed compensation method in a microgrid with unbalanced resistive load plus nonlinear load. (a) Output voltages and currents of DG1. (b) Output voltages and currents of DG2.

The auxiliary control is performed selectively for the main PCC voltage harmonics. Compensation reference of each harmonic (Ch± αβ for hth voltage harmonic) is generated separately and then, all of the compensation references are added together.

VI. CONCLUSION

This paper discusses an enhanced power sharing scheme for islanding microgrids. The proposed method utilizes the frequency droop as the link to compensate reactive, imbalance, and harmonic power sharing errors. The proposed method utilizes the selective virtual impedance loop, the local voltage unbalance and harmonics compensation block, and the auxiliary selective compensation of PCC voltage characteristic harmonics in a microgrid to compensate the reactive, unbalance, and the harmonic power sharing errors. In the primary control, the selective virtual impedance at the fundamental positive sequence, fundamental negative sequence, and harmonic frequencies are adopted to enhance the power sharing of reactive, unbalance and harmonic power between the DG units. The fundamental positive-sequence real and reactive powers are used by the power controllers to generate the references of the DG output voltage amplitude and phase angle. The feasibility of the proposed method is obtained by simulation results from a low-power three-phase micro grid with two parallel DG units with the same power rating

REFERENCES

[1] F. Blaabjerg, R. Teodorescu, M. Liserre, and V. A. Timbus, "Overview of control and grid synchronization for distributed power generation systems," IEEE Trans. Ind. Electron., vol. 53, no. 5, pp. 1398–1409, Oct. 2006.

[2] H. Han, X. Hou, J. Yang, J. Wu, M. Su, and J. M. Guerrero, "Review of power sharing control strategies for islanding operation ofACmicrogrids," IEEE Trans. Smart Grid, vol. 7, no. 1, pp. 200–215, Jan. 2016.

[3] J. M. Guerrero, J. C. Vasquez, J. Matas, M. Castilla, L. G. D. Vicu˜na, and M. Castilla, "Hierarchical control of droop-controlled AC and DC microgrids-A general approach toward standardization," IEEE Trans. Ind. Electron., vol. 58, no. 1, pp. 158–172, Jan. 2011.

[4] Y. Han, P. Shen, X. Zhao, and J. M. Guerrero, "Control strategies for islanded microgrid using enhanced hierarchical control structure with multiple current-loop damping schemes," IEEE Trans. Smart Grid, doi: 10.1109/TSG. 2015. 2477698.

[5] Q. Shafiee, J. M. Guerrero, and J. C. Vasquez, "Distributed secondary control for islanded microgrids—A novel approach," IEEE Trans. Power Electron., vol. 29, no. 2, pp. 1018–1031, Feb. 2014.

[6] H. Mahmood, D. Michaelson, and J. Jiang, "Accurate reactive power sharing in an islandedmicrogrid using adaptive virtual impedances," IEEE Trans. Power Electron., vol. 30, no. 3, pp. 1605–1617, Mar. 2015.

[7] I.U.Nutkani, P.C. Loh, and F.Blaabjerg, "Droop scheme with considering of operating cost," IEEE Trans. Power Electron., vol. 29, no. 3, pp. 1047–1052, Mar. 2014.

[8] D. De and V. Ramanarayanan, "Decentralized parallel operation of inverters sharing unbalanced and nonlinear loads," IEEE Trans. Power Electron., vol. 25, no. 12, pp. 3015–3025, Dec. 2010.

[9] Y. W. Li and C. N. Kao, "An accurate power control strategy for power electronics-interfaced distributed generation units operating in a lowvoltage multibus microgrid," IEEE Trans. Power Electron., vol. 24, no. 2, pp. 2977–2988, Dec. 2009.

[10] C. N. Rowe, T. J. Summers, R. E. Betz, D. J. Cornforth, and T. G. Moore, "Arctan power—frequency droop for improvedmicrogrid stability," IEEE Trans. Power Electron., vol. 28, no. 8, pp. 3747–3759, Aug. 2013.

[11] R. H. Lasseter et al., "CERTS microgrid laboratory test bed," IEEE Trans. Power Del., vol. 26, no. 1, pp. 325–332, Jan. 2011.

[12] Q. Shafiee, J. M. Guerrero, and J. C. Vasquez, "Distributed secondary control for islanded microgrids—A novel approach," IEEE Trans. Power Electron., vol. 29, no. 2, pp. 1018–1031, Feb. 2014.